J Mol Med
DOI 10.1007/s00109-008-0396-1

ORIGINAL ARTICLE

Lovastatin induces apoptosis of k-ras-transformed thyroid cells via inhibition of ras farnesylation and by modulating redox state

Chiara Laezza · Laura Fiorentino · Simona Pisanti · Patrizia Gazzerro · Michele Caraglia · Giuseppe Portella · Mario Vitale · Maurizio Bifulco

Received: 4 February 2008 / Revised: 1 August 2008 / Accepted: 4 August 2008

Abstract Transformation of thyroid cells with either K-ras or H-ras viral oncogenes produces cell types with different phenotype and different response to the inhibition of the prenylation pathway by 3-hydroxy-3-methylglutaryl-CoA reductase or farnesyltransferase inhibitors. These inhibitors induce apoptosis in K-ras-transformed FRTL-5 cells (FRTL-5-K-Ras) whereas cell cycle arrest is induced in H-ras-transformed FRTL-5 (FRTL-5-H-Ras). In FRTL-5-K-Ras cells, the product of K-ras gene is implicated in the scavenging of reactive oxygen species (ROS) through the activation of extracellular-signal-regulated kinase (ERK)1/2 kinases. We observed that lovastatin blocked ras activation through inhibition of farnesylation and induced apoptosis, increasing ROS levels through inhibition of ERK1/2 signaling and Mn-SOD expression. Lovastatin-induced apoptosis was due to intracellular ROS increase since both, the antioxidant compound pyrrolidinedithiocarbamate or the SOD-mimetic compound, antagonized apoptosis. Moreover, both p38 mitogen-activated protein kinase and nuclear factor κB pathways, activated as a consequence of high ROS levels, are involved in the apoptotic effect, indicating that cell death induced by lovastatin was dependent on oxidative stress. Lovastatin antitumor efficacy in K-ras-dependent thyroid tumors was further confirmed in vivo, proposing a new therapeutic strategy for those tumor diseases that are sustained by an inappropriate K-ras expression.

Keywords RAS · Thyroid · Lovastatin · Farnesylation

Abbreviations

ROS	reactive oxygen species
PDTC	pyrrolidinedithiocarbamate
GEFs	guanosine exchange factors
FTase	farnesyltransferase
HMG-CoA	3-hydroxy-3-methylglutaryl-CoA
MnTMPyP	Mn(III)tetrakis(1-methyl-4-pyridyl)porphyrin
Mn-SOD	Mn-superoxide dismutase

Ras proteins are involved in regulating many cellular processes, including proliferation, differentiation, and apoptosis [1–2]. Based on their origin, three forms of ras oncogene, namely K-ras, H-ras, and N-ras, have been detected. One way used by ras family proteins to regulate cell proliferation is the modulation of redox signals. It is

C.L. and L.F. contributed equally to this work.

C. Laezza
IEOS, CNR,
Naples, Italy

C. Laezza · G. Portella
Department of Cellular and Molecular Biology
and Pathology "L. Califano",
University of Naples Federico II,
Naples, Italy

L. Fiorentino · S. Pisanti · P. Gazzerro · M. Bifulco (✉)
Department of Pharmaceutical Sciences, University of Salerno,
84084 Fisciano, Salerno, Italy
e-mail: maubiful@unisa.it

M. Caraglia
Experimental Pharmacology Unit,
National Institute of Tumours Fondazione "G. Pascale" of Naples,
Naples, Italy

M. Vitale
Department of Molecular and Clinical
Endocrinology and Oncology,
University of Naples Federico II,
Naples, Italy

well established that rac1, an essential component of the reactive oxygen species (ROS)-producing NADPH oxidase, is downstream of ras which can therefore modulate intracellular ROS levels [3]. However, despite their stringent sequence homology, K-ras, H-ras, and N-ras can display different effects on the generation of ROS. In detail, K- and H-ras genes have been shown to exert opposing functions in the regulation of redox signals, since H-ras protein can increase ROS production, while K-ras decreases ROS levels by acting via the extracellular-signal-regulated kinase (ERK1/2) kinases on different intracellular targets [4]. Activation of the ras oncogene product p21 requires the linkage of a farnesyl group, allowing the protein anchorage to the cell membrane and the subsequent interaction with guanosine exchange factors located in receptor-associated complexes [5–6]. Some ras family proteins such as K-ras can be alternatively activated through the addition of a geranylgeranyl moiety. The farnesylation process has an important role in the determination of the transformed phenotype [7].

Mutations involving codon 61 of *H-ras and N-ras* have been reported with variable frequency in thyroid neoplasms. Ras mutations are more common in iodine-deficient than iodine-sufficient areas and in lesions with follicular architecture (including follicular carcinoma and follicular variant papillary thyroid carcinoma) than in typical papillary thyroid carcinoma [8]. On the basis of the involvement of ras in thyroid carcinogenesis, we have evaluated the role of ras proteins in the regulation of the isoprenoid pathway in FRTL-5 thyroid cells and we have found that it is deeply altered upon transformation with v-K-*ras* [9]. K-ras, different from H-ras, induces metabolic changes in the isoprenoid pathway resulting in a preferential farnesylation and subsequent functional activation of the oncogene product. This effect is mainly produced by downregulating mevalonate kinase and inducing the activity of farnesyltransferase (FTase) enzyme. In line with these data, we also observed an enhanced activity of FTase in colon tumor tissue, correlated to tumor location, histological grading, and K-ras mutation [9]. On the basis of these data, the specific inhibition of isoprenylation processes could be a useful tool to block K-ras both transforming and growth-regulating activity. Pharmacological compounds inhibiting enzymes involved in protein isoprenylation have been proposed as anticancer tools [10–11]. Among these, lovastatin, an irreversible inhibitor of 3-hydroxy-3-methyl-glutaryl-CoA (HMG-CoA) reductase, used in clinic to treat hypercholesterolemia through blocking the mevalonate biosynthesis pathway, has been shown to induce apoptosis in several tumor types [12–15]. The mechanism of apoptosis induced by lovastatin and its correlation with ras oncogene expression are poorly understood so far.

We previously reported that the inhibition of prenylation by lovastatin induced apoptosis in human neoplastic thyroid cells [16].

In the present manuscript, to investigate the role of ras oncogene in the cytotoxicity induced by prenylation inhibitors, we used as a model K-ras- or H-ras-transformed thyroid cells. We analyzed whether the proapoptotic effect of this statin was related to an interference with the p21-ras-mediated activation of pathways leading to oxidative stress.

Materials and methods

Materials, drugs, and antibodies

Lovastatin was a generous gift of Dr. A.W. Alberts (Merck Sharp and Dohme Research Laboratories, West Point, PA, USA); PD98059 and SB203580 were purchased from Calbiochem (La Jolla, CA, USA). Protease inhibitors (aprotinin and leupeptin) were purchased from Roche Diagnostics GmbH (Mannheim, Germany); protein electrophoresis reagents were from Bio-Rad laboratories (Hercules, CA, USA), Western blotting and enhanced chemiluminescence (ECL) reagents were from GE Healthcare (Milano, Italy). All other chemicals were from Sigma-Aldrich. Cell culture reagents were obtained from Gibco (Grand Island, NY, USA). Anti-ERK1/2 antibodies were purchased from Chemicon (Temecula, CA, USA); antibodies were from Santa Cruz Biotechnology Inc. (CA, USA). FTI-277 and GGTI were purchased from Merck (Darmstadt, Germany). Mevalonate and pyrrolidinedithiocarbamate were purchased from Sigma-Aldrich (St. Louis, MO, USA). All the substances were used at the most efficacious doses experimentally evaluated. Inducible expression vector coding for a dominant-negative mutant of ras (ras $p21^{N17}$) was a kind gift of Prof G. Vecchio.

Cell lines

FRTL-5 (ATCC CRL 8305) is a differentiated rat thyroid cell line; FRTL-5-K-Ras and FRTL-5-H-Ras cells, derived from FRTL-5 stably transfected with v-K-ras or v-H-ras oncogene, respectively, were kindly provided by Prof. G. Vecchio. FRTL-5-H-Ras and FRTL-5-K-Ras cells were grown in Coon's modified Ham's F12 medium supplemented with 5% calf serum. Photos were acquired in light microscopy at ×10 magnification.

Assessment of cell cycle and apoptosis by propidium iodide labeling

The induction of apoptosis by different treatments was assessed as the percentage of hypodiploid sub-G1 peak

measured by flow cytometry. Briefly, the cells were incubated for 24 h with the indicated drugs, then collected, washed with phosphate-buffered saline (PBS), and resuspended in 300 μl of PBS. Seven-hundred microliters of ethanol 70% were added slowly to the cells on a vortex and kept at −20°C overnight. Propidium iodide (PI; 10 μg/ml) in PBS containing 100-U/ml DNase-free RNase A was added to the cells. After 4 h at room temperature, cells were subjected to flow cytometric analysis. Data acquisition and analysis were performed in a Becton Dickinson FACSCalibur flow cytometer using CellQuest software.

DNA fragmentation assay

For detection of apoptosis by the DNA fragmentation assay, treated cells were harvested, resuspended in 0.5 ml of lysis buffer (20 mM ethylenediaminetetraacetic acid (EDTA), 10 mM Tris pH 8.0, 200 mM NaCl, 0.2% Triton X-100, and 100 μg/ml Proteinase K) and incubated for 1.5 h in a 37°C incubator. The samples were centrifuged (12,000 rpm) in room temperature for 5 min. The supernatant was transferred to a new Eppendorf tube and equal volumes of isopropanol and 25 μl of 4 M NaCl (100 mM final concentration) were added, followed by overnight incubation of the samples at −20°C. DNA was acquired by centrifugation of the samples, washed, dried, and dissolved in 30 μl TE (10 mM Tris–1 mM EDTA, pH 8.0) buffer. Five micrograms of DNA were loaded on each lane of 1.5% agarose gel.

Fluorescent measurement of intracellular ROS

Cells were trypsinized, collected in polystyrene tubes, and washed three times with 137 mM NaCl, 3.7 mM KCl, 10 mM Na_2HPO4, 1.76 mM KH_2PO4, pH 7.5 (PBS). Cells numbering 1×10^6 were suspended in 2 ml of PBS and incubated with 10 μM of 5,6-carboxy-2′,7′-dichlorofluorescein diacetate (DCHFDA; Molecular Probes, Eugene, OR), for 1 h at 37°C and kept in DCHFDA continuously thereafter. Cells were analyzed with fluorescent-activated cell sorting (FACS) analysis with excitation and emission setting of 495 and 525 nm, respectively.

Western blot analysis

Subconfluent monolayer of cells were washed with PBS and then lysed in a lysis buffer containing 20 mM 4-(2-hydroxyethyl)-1-piperazineethanesulfonic acid (HEPES) pH 7.5, 150 mM NaCl, 10% glycerol, 1% Triton X-100, supplemented with a mixture of protease inhibitors. Equal amounts of total proteins (50 μg) were resolved on 12% sodium dodecyl sulfate-polyacrylamide gel electrophoresis (SDS-PAGE). After immunoblotting of gels onto polyvinylidene difluoride sheets (Millipore), filters were blocked for 1 h at room temperature with 10% nonfat dry milk (Bio-Rad) in TBS-T buffer (10 mM Tris–HCl pH 8, 0.1% Tween 20, 150 mM NaCl). The filters were then incubated with the specific primary antibodies as showed in the figures followed by horseradish peroxidase (HRP)-conjugated secondary antibodies. Blots were revealed by ECL system (GE Healthcare). Immunoreactive bands were quantified using Quantity One I-D analysis software (Bio-Rad).

Measurement of cell viability

About 5×10^3 FRO cells/well were seeded in 96-well culture plates and incubated for 24 h at 37°C with 10 μM lovastatin. Cell survival was examined by using 3-(4,5-dimethylthiazol-2-yl)-5-(3-carboxymethoxyphenyl)-2-(4-sulphophenyl)-2H-tetrazolium, inner salt (MTS), and an electron coupling reagent (phenazine methosulfate), according to manufacturer's instructions (Promega).

Affinity precipitation of Ras

The cells were lysed in the Mg^{2+} buffer containing 20 mM HEPES, pH 7.5, 150 mM NaCl, 1% Igepal CA-630, 10 mM MgCl2, 1 mM EDTA, and 2% glycerol. Then, 10 μl Ras Binding Domain conjugated to agarose (Cell Signaling Technology, MA, USA) were added to 1 mg of cell lysate and the resulting mixture was incubated overnight with gentle rocking at 4°C. The agarose beads were collected by microcentrifugation at $14{,}000\times g$ for 5 s and washed three times with Mg^{+2} buffer. The agarose beads were boiled for 5 min in 2X Laemmli sample buffer and collected by a microcentrifuge pulse. The supernatants were run on 12% SDS-PAGE; then, the proteins were electrotransferred on a nitrocellulose film. The nitrocellulose was incubated overnight with 1 μg/ml of anti-Ras Mab, clone RAS1,0 and with a secondary Mab, a goat α-mouse HRP-conjugated immunoglobulin G, for 1 h. The film was washed with TBS/0.05% Tween 20 and detected by ECL, chemiluminescence technique (Amersham).

Electromobility shift assay

Double-stranded oligonucleotides containing the NF-κB recognition sequence (5′-CAACGGCAGGGGAATCTC CCTCTCCTT-3′) was end-labeled with ^{32}P-adenosine triphosphate. Nuclear extracts containing 5 μg of protein were incubated for 15 min with radiolabeled oligonucleotides (2.5 to 5.0×10^4 cpm) in a reaction buffer as previously described [17]. The specificity of the NF-κB–DNA binding was determined by a competition reaction in

which a 50-fold molar excess of unlabeled wild-type, mutant, or Sp-1 oligonucleotide was added to the binding reaction 15 min before the radiolabeled probe. Nuclear protein–oligonucleotide complexes were resolved by electrophoresis on a 6% nondenaturing polyacrylamide gel in 1× TBE (Tris borate–ethylenediaminetetraacetic acid) buffer at 150 V for 2 h at 4°C. The gel was dried and autoradiographed with intensifying screen at −80°C for 20 h. Subsequently, the relative bands were quantified by densitometric scanning of the X-ray films with a GS-700 Imaging Densitometer (Bio-Rad) and a computer program (Molecular Analyst; IBM).

Animals and in vivo tumorigenicity assay

All animal studies have been carried out in accordance with the National Institutes of Health (NIH) Guide for the care and the use of laboratory animals, and protocols were approved by the local Institutional Animal Care and Use Committee. Adult female nude mice (CD1) were purchased from the Charles River Laboratories s.r.l. The mice were housed in polyethylene cages, in rooms maintaining a controlled temperature on a 12-h light–dark cycle and given rodent chow and water ad libitum. The experiments were performed in 6-week-old male athymic mice. Briefly, FRTL-5-K-Ras cells (suspension of 0.2 ml containing 1×10^6 cells) were injected subcutaneously (s.c.) into the right flank of 30 athymic mice. When tumors had developed to ~0.2 cm^3, groups of ten mice each were injected intraperitoneally (i.p.) with either vehicle alone or with 50 mg/kg lovastatin three times a week for 4 weeks. Individual body weights were recorded weekly. Animals were checked weekly and tumor volume was measured with calipers every other day until the animals were killed. Tumor volumes (V) were calculated by the formula of rotational ellipsoid: $V = A \times B\ 2/2$ (A = axial diameter, B = rotational diameter). During the treatment, none of the mice showed signs of wasting or other visible indications of toxicity. Furthermore, lovastatin-used dose showed no detectable reduction of the spontaneous activity, as we observed unimpaired locomotion of the treated mice. After 4 weeks, animals were sacrificed.

Statistical analysis

All data were presented as means ± SD. Statistical analysis was performed using one-way analysis of variance (ANOVA). In the case of a significant result in the ANOVA, Student T test was used for dose–response curve and Bonferroni's test for post hoc analysis for all other experiments. A p value less than 0.05 was considered statistically significant.

Results

Effect of lovastatin on cell cycle of FRTL-5-K-Ras and FRTL-5-H-Ras cells

Lovastatin, a competitive inhibitor of HMG-CoA reductase, blocks DNA synthesis and proliferation of thyrotropin-primed FRTL-5 rat thyroid cells [18]. Two other cell lines, FRTL-5-K-Ras and FRTL-5-H-Ras, derived from FRTL-5 upon transformation by active v-K-*ras* or v-H-*ras* oncogenes, respectively, were tested for their response to lovastatin. In both cell lines, transformation resulted in uncontrolled proliferation, loss of thyroid-specific gene expression, and tumorigenicity [19–20].

We evaluated the effects of 10 μM lovastatin on cell shape and growth of FRTL-5-K-Ras and FRTL-5-H-Ras cells, finding that, while cell shape change was only minimal in FRTL-5-H-Ras, dramatic cell morphology changes were observed in FRTL-5-K-Ras cells. By 12-h treatment, FRTL-5-K-Ras cells were still adherent to the plate but their shape changed from flat to round. By 24 h, the majority of the cells were detached and floating in the medium (data not shown). FRTL-5-H-Ras cells became more rounded during the treatment and remained adherent to the plate (data not shown). Growth response curves over a range (0–10 μM) of lovastatin concentrations for all the thyroid cell lines used are shown in Fig. 1a. Lovastatin inhibited in a dose-dependent manner the proliferation of FRTL-5-K-Ras without a significant effect in the other cell lines used. An increase of dead cells was at the same time

Fig. 1 Apoptotic effect of lovastatin on FRTL-5-K-Ras cells. **a** Effect of lovastatin on cell number. A total of 2×10^4 cells were seeded and cultured for 24 h. Then, lovastatin was added at the indicated doses and the number of adherent cells was calculated after 24 h. Shown is the mean ± SD of triplicates. The experiment was conducted twice. **b** FACS analysis after propidium iodide staining of FRTL-5-H-Ras (*a* and *b*) cells and FRTL-5-K-Ras (*c* and *d*) cells treated with 10 μM lovastatin for 24 h. In the *table* is reported the mean percentage of cells in each phase of the cell cycle (*Apo*, apoptosis). *a* and *c*, untreated cells; *b* and *d*, lovastatin (10 μM, 24 h). **c** The graph shows the percentage of apoptosis measured as hypodiploid DNA content for FRTL-5-K-Ras cells treated with different concentrations of lovastatin for 24 h. **d** The internucleosomic DNA fragmentation was assessed in FRTL-5-K-Ras cells as described in "Materials and methods." **e** Western blot analysis of total and cleaved caspase 3 (17 kDa). Equal amounts of protein were loaded in each *lane*. **f** The percentage of apoptotic cells evaluated by FACS analysis after propidium iodide labeling of Ats cells. *Ctr*, untreated cells; *Lova*, 24 h lovastatin 10 μM. **g** The percentage of apoptotic cells evaluated by FACS analysis after propidium iodide labeling of FRTL-5-K-Ras cells treated with lovastatin, farnesyl-transferase inhibitor FTI-277 (*FTI*) or geranylgeranyl-transferase inhibitor (*GGTI*), negative-dominant mutant of ras (*N17*) and with the MAPK inhibitor PD98059 (*PD*). The experiments were performed at least three different times and the results were always comparable. Statistical significance versus control; $^{**}p<0.01$; $^{*}p<0.05$

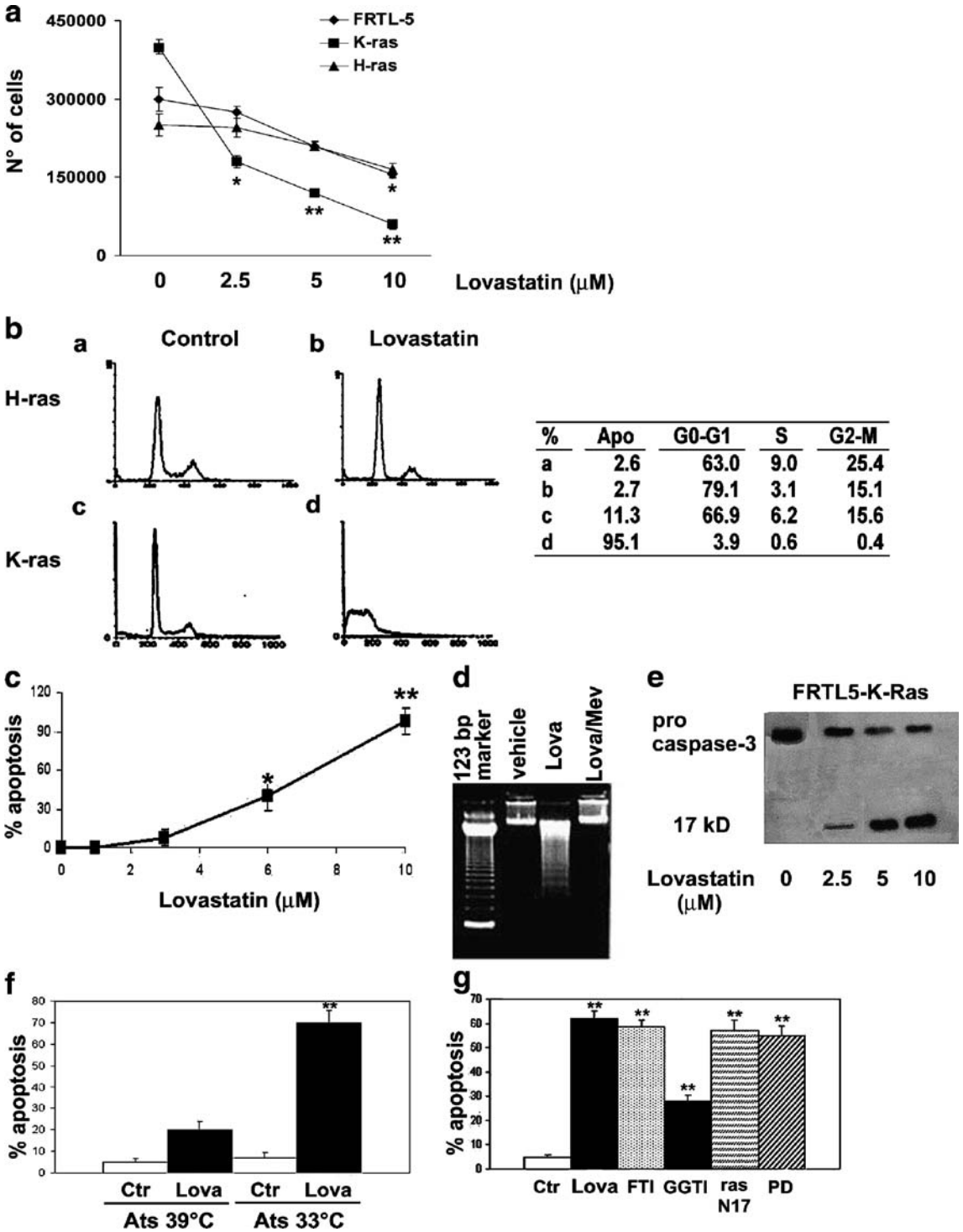

observed (data not shown). Therefore, we decided to evaluate the apoptotic effects of lovastatin by FACS analysis after PI labeling. We found that the treatment with lovastatin for 12 h had null or little effects on apoptosis of FRTL-5-K-Ras cells (data not shown). However, by 24 h treatment, almost 100% of FRTL-5-K-Ras cell population was hypodiploid (Fig. 1b, panels c and d), while FRTL-5-H-Ras cells did not show a significant increase of hypodiploid cell number but only cell accumulation in the G1 phase of the cell cycle (Fig. 1b, panels a and b). Treatment with lovastatin as early as 2 h blocked DNA synthesis in FRTL-5-H-Ras cells, thus increasing the number of cells in G1 phase and decreasing the number of cells in S phase (data not shown). The number of FRTL-

5-K-Ras cells with hypodiploid DNA content, evaluated after 24 h of treatment by flow cytometry, increased in a dose-dependent manner, attaining 100% at 10 μM lovastatin concentration and 50% at a concentration of 7.5 μM (Fig. 1c). Loss of diploid DNA cell content started at 12 h from the beginning of lovastatin treatment and continued in a time-dependent manner (data not shown).

A further demonstration that the loss of DNA cell content induced by lovastatin was due to apoptosis was obtained by DNA ladder analysis evaluated by agarose gel electrophoresis that displayed the characteristic DNA fragmentation (Fig. 1d). A molecular assessment of apoptosis induction was performed by evaluating, by Western blot analysis, the levels and the cleavage into the active form of pro-caspase 3. We observed a dose-dependent increase in the activation of caspase 3 (Fig. 1e). Interestingly, the proapoptotic effect of lovastatin was prevented by the addition of mevalonate (0.7 mM; Fig. 1d), whereas the same analysis performed on FRTL-5-H-Ras cells did not show any DNA degradation (data not shown). To further confirm that the induction of apoptosis by lovastatin was an effect specifically dependent on K-ras transformation of thyroid cells, we used a different FRTL-5-cell-derived line, Ats that is transformed with a Kirsten-murine sarcoma virus variant carrying a temperature-sensitive v-K-*ras* allele [21]. Lovastatin had no significant effect on cells grown at 39°C, a nonpermissive temperature for p21 ras activity, whereas apoptosis was rapidly induced by lovastatin at the permissive temperature of 33°C (Fig. 1f).

Role of farnesylation in lovastatin-induced apoptosis in K-ras-transformed cells

Lovastatin is an inhibitor of HMG-CoA reductase and affects FTRL-5 cell proliferation mainly through an indirect inhibition of protein farnesylation [18]. In order to identify the mechanisms responsible for the induction of apoptosis in cells expressing an active form of K-ras oncogene, we determined whether both farnesylation inhibition and K-ras were required for the observed effect and, thereafter, investigated the downstream mitogen-activated protein kinase (MAPK) pathway activated by ras. To determine whether inhibition of protein prenylation was responsible for apoptosis induced by lovastatin in FRTL-5-K-Ras cells, we used farnesyl- or geranylgeranyl-protein transferase inhibitors (FTI-277 or GGTI-298, respectively; Fig. 1g). Treatment with 40 μM of GGTI-298 for 16 h induced apoptosis only in a small percentage of cells, whereas FTI-277 completely reproduced the effect induced by lovastatin, thus suggesting a main role of farnesyl-protein transferase inhibition (Fig. 1g). Furthermore, transfection of FRTL-5-K-Ras cells with a construct expressing a negative-dominant mutant of ras protein produced effects comparable to those caused by lovastatin or FTI-277. These data confirmed the hypothesis that inhibition of HMG-CoA reductase by lovastatin occurred through the inactivation of ras protein due to the inhibition of its farnesylation (Fig. 1g).

Effects of lovastatin on ras-dependent survival signal transduction pathways

Since an important mechanism for ras activation is represented by its isoprenylation, we evaluated the effects of lovastatin on ras activity in FRTL-5-K-Ras cells. We found that lovastatin did not induce changes in ras expression as evaluated by Western blotting analysis (Fig. 2a). However, lovastatin induced about 60% decrease of ras activity as evaluated by affinity precipitation with the agarose-conjugated minimal binding domain of raf-1 followed by Western blotting analysis for ras (Fig. 2a,b).

We also evaluated the effects of lovastatin on the ras-dependent MAPK pathway, ERK1/2 and p38 MAPK, playing a relevant role in cell survival. We found that lovastatin strongly decreased ERK1/2 activities after 6 h of treatment as evaluated by Western blot assay using a Mab raised against the phosphorylated–activated isoforms of the protein (Fig. 2a).

On the other hand, at the same experimental conditions, lovastatin did not induce substantial changes of ERK1/2 expression, thus suggesting a direct effect on enzyme activation induced by the upstream regulators more than on enzyme expression–content. Moreover, the ERK1/2 inhibitor PD98059 (20 μM, 24 h) exerted a proapoptotic activity comparable to that of lovastatin in FRTL-5-K-Ras cells (Fig. 1g). These data suggest that apoptosis induced by inhibition of k-ras could be mediated by inhibition of ERK1/2.

We concomitantly observed a strong increase of p38 MAPK phosphorylation in lovastatin-treated cells compared to control cells at 24 h (Fig. 2a, b), while total p38 MAPK levels were not changed (Fig. 2a). Therefore, lovastatin-induced apoptosis is associated with inhibition of ERK1/2 and activation of p38 MAPK, both correlated to apoptosis onset in several cell models.

Effect on ROS levels in FRTL-5-K-Ras cells

It has been previously reported that MAP kinases negatively regulate ROS production and their inhibition through K-ras inhibitors leads to an increase in ROS production in K-ras-transformed fibroblasts [4]. Therefore, we analyzed the effect of lovastatin on ROS levels in FRTL-5-K-Ras cells. ROS production, evaluated by flow cytometry as fluorescence of the oxidation-sensitive probe DCHFDA,

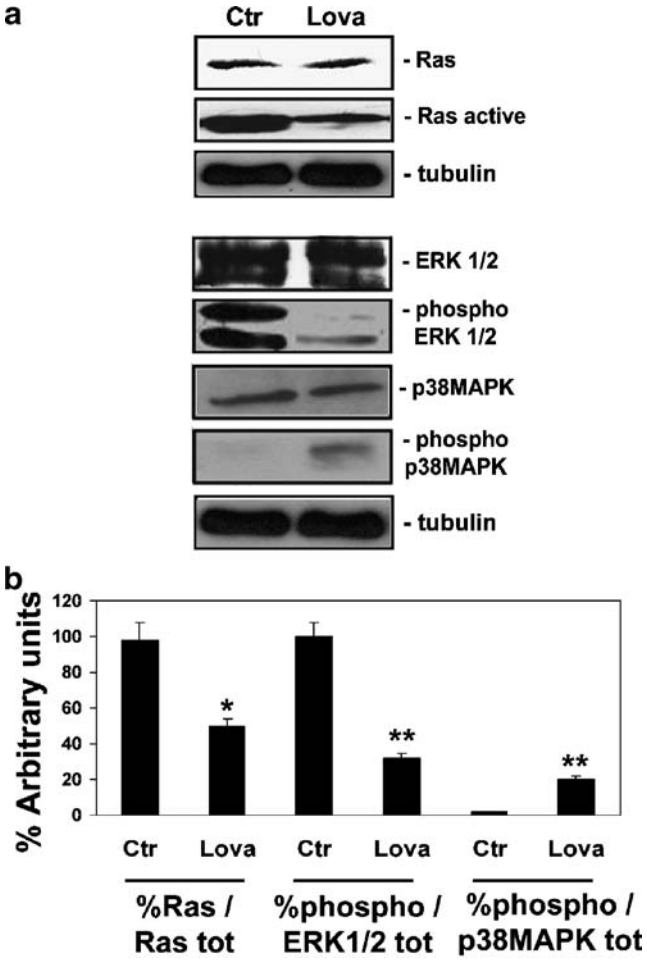

Fig. 2 Effect of lovastatin on ras activity and on the phosphorylation status of ERK1/2 and p38 MAPK. **a** Western blot assay for the expression of the total ras protein. Affinity precipitation of ras performed with the minimal binding domain of raf-1 conjugated with agarose microspheres for the evaluation of ras activity as described in "Materials and methods." Determination of the expression and phosphorylation of ERK1/2 and p38 MAPK. Filters were stripped and reprobed with tubulin as loading control. **b** Laser scanner of the bands associated to ras activity, pErk and p38 MAPK phosphorylation status. The intensities of the bands were expressed as percent arbitrary units and calculated as mean ratio (±SD) of control protein (tubulin). Statistical significance versus control; $^{**}p<0.01$; $^{*}p<0.05$. *Ctr*, untreated cells; *Lova*, 24 h lovastatin 10 μM. The experiments were performed at least three different times and the results were always comparable

was increased in cells treated with lovastatin for 24 h (Fig. 3a). Similar effects were produced by treating cells with either the ERK1/2 inhibitor PD98059 or the farnesyl-protein transferase inhibitor, FTI-277, or by cell transfection with the plasmid ras^{N17} expressing a dominant-negative ras mutant protein (Fig. 3a). In order to determine whether lovastatin-induced apoptosis was mediated by increased intracellular ROS levels, we used PDTC, an antioxidant molecule, in cells treated with lovastatin and apoptosis was measured by FACS analysis. We found that 0.5–1 mM PDTC almost completely inhibited apoptosis induced by lovastatin (Fig. 3b).

The primary enzymatic antioxidant system in the cell is represented by SOD isoenzymes. Therefore, we measured by Western blot the levels of the Mn-SOD enzyme, which has been previously reported to be stimulated by K-ras oncogenic signaling through ERK1/2-dependent pathway [4]. Lovastatin treatment (10 μM) induced a time-dependent reduction in Mn-SOD levels and the inhibitory effect was prevented by PD98059 pretreatment, suggesting the involvement of ERK1/2 in this effect (Fig. 3c). Mn(III) tetrakis(1-methyl-4-pyridyl)porphyrin (MnTMPyP), a superoxide dismutase–catalase mimetic that replicates Mn-SOD effects, was assessed on lovastatin-induced apoptosis of FRTL-5-K-Ras cells. MnTMPyP reversed the proapoptotic effect of lovastatin, suggesting the involvement of intracellular ROS (Fig. 3d). Furthermore, since p38 MAPK pathway seems to be implicated in lovastatin apoptosis, we tested also the effect on apoptosis of p38 MAPK inhibitor SB203580. We observed that SB203580 also reverses the proapoptotic effect of lovastatin, thus suggesting that inactivation of K-ras by inhibitors of prenylation produced cell death by increasing the intracellular ROS levels (Fig. 3d).

Activation of NF-κB by lovastatin in thyroid FRTL-5-K-Ras cells

It is well known that an increase of ROS can induce the activation of NF-κB. Because lovastatin caused an induction of ROS inside the cells, we investigated the involvement of NF-κB in lovastatin-induced apoptosis. We found that a specific NF-κB-blocking peptide (SN18) was only partially able to antagonize lovastatin-induced apoptosis (Fig. 3d). The next step was to investigate if lovastatin was able to directly activate NF-κB in FRTL-5-K-Ras cells. We monitored the levels of the inhibitory subunit Iκ-Bα by Western blot and we found that Iκ-Bα levels decreased time-dependently after lovastatin treatment (Fig. 4a). In addition, we have found on FRTL-5-K-Ras cells that lovastatin likely caused the nuclear translocation of NF-κB suggesting its binding to DNA in a time-dependent manner as evaluated by electrophoretic mobility shift assay (Fig. 4b). Therefore, NF-κB is activated by lovastatin probably as a consequence of ROS induction.

In vivo antitumoral effect of lovastatin

In order to examine if the in vivo growth of K-ras-expressing tumor cells was impaired by lovastatin, athymic mice were s.c. inoculated with FRTL-5-K-Ras cells. The FRTL-5-K-Ras xenografts tumors were allowed to grow for 3 days. When tumors had developed to ~0.2-cm^3 volume,

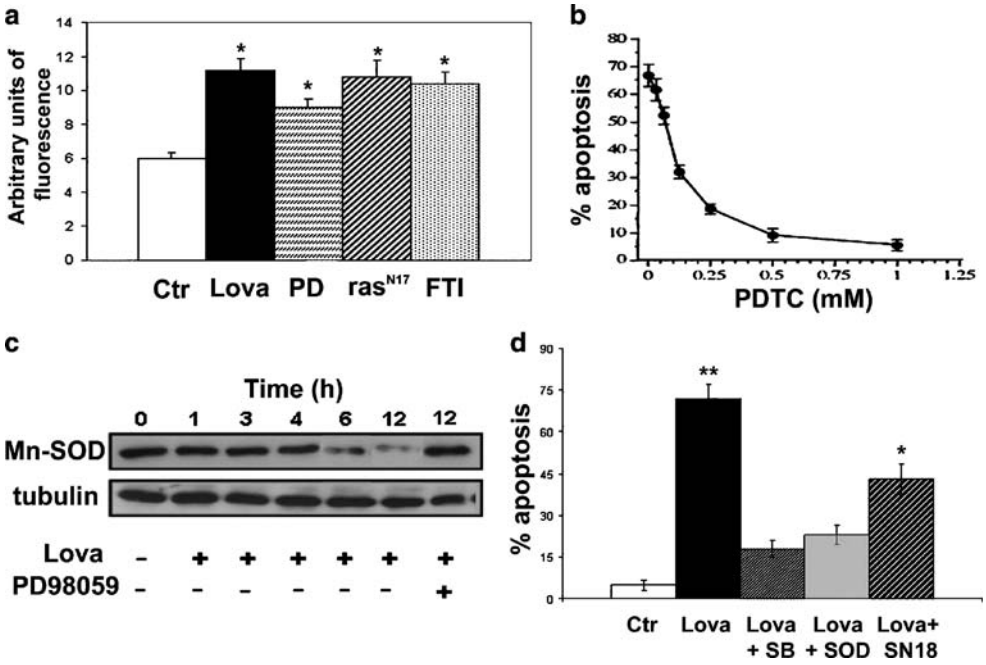

Fig. 3 Effect on ROS levels in FRTL-5-K-Ras cells. **a** DCF fluorescence of FRTL-5-K-Ras cells after treatment with lovastatin (*Lova*), ERK 1/2 inhibitor PD098059 (*PD*), negative-dominant mutant of ras (ras^{N17}), and farnesyl-transferase inhibitor FTI-277 (*FTI*) was evaluated as described in "Materials and methods." **b** The percentage of apoptotic cells evaluated by FACS analysis after propidium iodide labeling of FRTL-5-K-Ras cells treated with increasing doses of PDTC. **c** Western blot analysis for the expression of Mn-SOD. The *diagram* shows quantification of immunoreactive bands, calibrated to the intensity of the tubulin bands, and expressed as mean ± SD. **d** Apoptotic effect induced in FRTL-5-K-Ras cells by lovastatin (10 μM) alone and in combination with p38 MAPK inhibitor SB203580 (*Lova + SB*), SOD-mimetic compound MnTMPyP (*Lova + SOD*), or peptide blocking NF-κB (*Lova + SN18*). Cell death was assessed as the percentage of hypodiploid elements measured by FACS analysis after propidium iodide labeling. Statistical significance versus control: $^{**}p<0.01$; $^{*}p<0.05$. The experiments were performed in triplicates at least three different times and the results were always comparable

groups of ten mice each were injected i.p. with either vehicle alone or with 50 mg/kg lovastatin three times a week for 4 weeks. Interestingly, the concentration of lovastatin used in the present study for both in vitro and in vivo experiments corresponds to high dose of lovastatin for clinical setting as previously reported by others [22–23].

As shown in Fig. 5, approximately 16 days after the beginning of treatment, the average tumor volume in lovastatin-treated group was dramatically reduced if compared with control groups ($p<0.01$, Fig. 5a).

Within 4 weeks after tumor cell injection, in the control group, tumor volumes acquired dimensions leading to the need of sacrifice, pursuant to the ethical NIH Guide for the use of laboratory animals. The experiment was stopped at 4 weeks for treated and control groups. Tumor volumes in each group were compared: substantial reduction of tumor growth was observed in lovastatin-treated animals compared with the controls (Fig. 5a). Moreover, the treatment did not have any evident detrimental and toxic effect since the body weight of treated mice was the same to that of the control (Fig. 5b). Interestingly, the treatment with lovastatin induced a prolongation of mice survival. In fact, after 4 weeks, 75% of the mice have not still achieved a tumor volume more than 3 cm^3 (Fig. 5c).

Discussion

Sustained cell survival is an essential feature of the transformed phenotype and different mechanisms contribute to the suppression of apoptosis in different tumor types. Ras-induced tumorigenesis is accompanied by a number of biochemical changes, including the activation of the ERK MAP kinase (MAPK)-, PI3K-, and RalGDS-signaling pathways. In ras-transformed cells, oncogene activation can lead to the block of death pathways [1]. One element that critically influences cell survival is ROS intracellular levels [24], whose increase can produce an alteration of the mitochondrial membrane permeability and cell apoptosis [25]. High levels of ROS have been detected in several human cancer cell lines [26], as well as in human tumors from different tissues [27]. ROS have also been reported to mediate some biological effects of oncogenic H-ras, including malignant transformation [28]. H- and K-ras

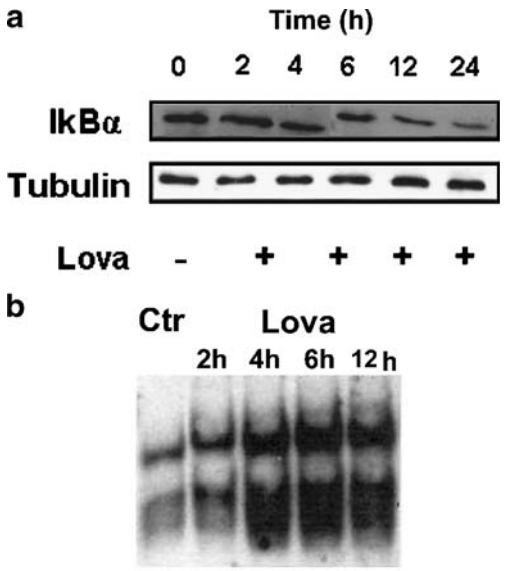

Fig. 4 Activation of NF-κB by lovastatin in FRTL-5-K-Ras thyroid cells. **a** Western blot assay for the expression of IkBα. The filter was stripped and reprobed with tubulin as loading control. **b** DNA binding activity of NF-κB in total extracts of FRTL-5-K-Ras cells treated with lovastatin up to 12 h

proteins differently modulate ROS levels: expression of H-ras increases ROS production by inducing the NADPH–oxidase system, whereas K-ras stimulates the scavenging of ROS by posttranscriptionally activating the mitochondrial antioxidant enzyme, Mn-SOD, via an ERK1/2-dependent pathway [4]. The mechanism underlying the opposing functions of H- and K-ras in ROS modulation is not completely understood and might be related to a different preferential intracellular localization of the two proteins [4]. The results presented in this report demonstrated a relationship between ROS-scavenging activity of K-ras and the regulation of apoptosis induced by prenylation inhibitor lovastatin in thyroid-transformed cells. Transformation of thyroid cells with K-ras or H-ras viral oncogenes produces cell types with different phenotype. v-K-*ras* caused a dramatic change in the pattern of prenylated proteins from the one observed in H-ras-transformed or nontransformed FRTL-5 cells, being the only ras oncogene product which farnesylated protein in K-ras-transformed cells [9]. Furthermore, the expression of a viral K-ras oncogene produced a different sensitivity of thyroid cells to the inhibition of the prenylation pathway, producing apoptosis rather than the cell cycle arrest, observed in normal or H-ras-transformed thyroid cells. In detail, in FRTL-5-K-Ras cells, inhibition of prenylation by lovastatin or by a specific inhibitor of FTase inhibited K-ras activation and its downstream effects such as ERK1/2 activation and ROS scavenging, leading to apoptosis. The increase of intracellular ROS levels necessary to apoptosis induced by lovastatin was accompanied by a time-dependent inhibition of Mn-SOD and confirmed by the reversion of lovastatin effect in these cells by MnTMPyP, a SOD-mimetic compound. Furthermore, levels of phosphorylated p38 MAPK were increased in response to lovastatin treatment, suggesting that activation of this MAPK is associated with induction or execution of apoptosis, with activation of caspase-3. A specific p38 MAPK inhibitor abrogated the effects of lovastatin on apoptosis, indicating that both ROS and p38 MAPK are necessary for lovastatin to have its

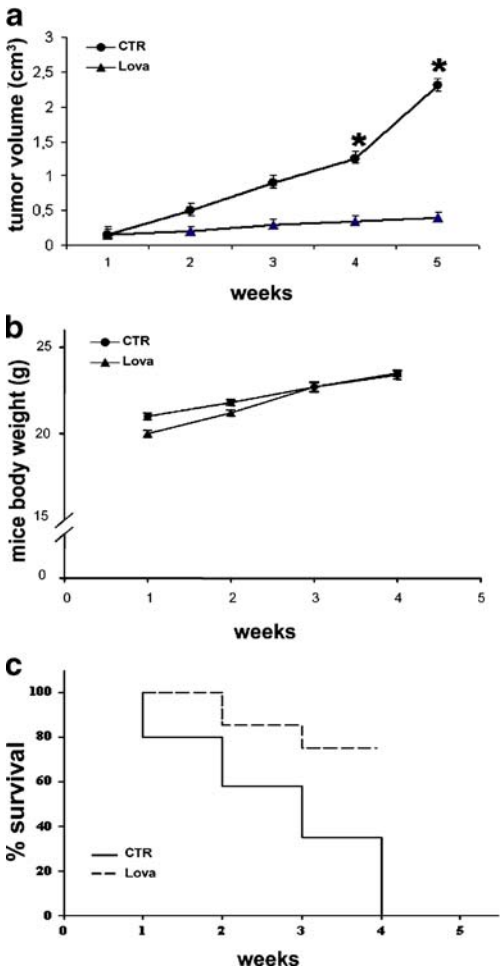

Fig. 5 Antitumor activity of lovastatin on established FRTL-5-K-Ras xenografts. Growth inhibition of FRTL-5-K-Ras xenografts (**a**) and body weight changes (**b**) of nude mice. FRTL-5-K-Ras cells (1×10^6) were s.c. injected in athymic mice as described in "Materials and methods." After 3 days, mice were administered with lovastatin (50 mg/kg) on days 2 and 5 weekly, for 4 weeks. *Points*, average tumor volume measured in each mouse of the group. Data were expressed as mean ± SD of $n=10$ animals each group. Differences in tumor volumes (**a**) after 4 weeks were significant (***$p<0.001$ by ANOVA followed by Bonferroni's test) between the control (*circles*) and lovastatin-treated groups (*triangles*). *Bars*, SDs. On the other hand, the differences in body weight did not reach statistical significance ($p>0.05$). **c** Kaplan Meyer curves representing the survival of Control (*solid line*) and Lova-treated (*dashed line*) mice

proapoptotic effects. p38 MAPK may also antagonize malignant transformation induced by all oncogenic ras forms [29]. It has recently been reported that p38 MAPK specifically modulates malignant transformation induced by oncogenes that produce ROS [30]. Interestingly, since highly tumorigenic cancer cells can override this p38 function uncoupling its activation from oxidative stress production, its induction by a chemotherapy drug could be very useful. In our model, p38 MAPK could be probably activated as a consequence of the high ROS levels accumulated in the cells after lovastatin inhibition of K-ras oncogene signaling pathways and of Mn-SOD, rather than a direct target of p38 MAPK signaling. In our experimental model, Mn-SOD expression was reduced by LOVA treatment even if a significant ROS elevation was also recorded. In fact, ROS activates the nuclear factor E2-related factor-2 (Nrf2) that is a member of CNC (cap 'n' collar) family of b-Zip transcription factors and is an indispensable positive regulator of many antioxidant and phase II detoxifying enzymes [31]. On activation by oxidative or electrophilic stress, Nrf2 protein stabilizes, translocates to the nucleus, heterodimerizes with small Maf proteins, and binds to the so-called antioxidant response element, a common regulatory element found in the 5′-flanking regions of antioxidant and detoxification enzymes including SOD [32]. On the other hand, eukaryotic cells can protect themselves from oxidative stress through the induction of SOD expression via a ras-dependent pathway [33]. On the basis of these considerations, the decreased Mn-SOD expression found in our conditions and occurring together with ROS elevation could be, at least in part, explained by the block of ras activity induced by lovastatin.

ROS are emerging as key effectors in signal transduction and this role is especially evident in the pathways leading to programmed cell death. Another pathway that is under ROS-mediated control in some systems is that leading to activation of NF-κB, which is a central regulator of cell survival, being either as a proapoptotic or as an antiapoptotic protein depending on cell type and apoptotic inducers [34]. Our data suggest that lovastatin induced NF-κB transcriptional activity in FRTL-5-K-Ras cells, probably as a consequence of ROS induction, suggesting a possible role of this factor worth to be investigated. There is also evidence that p38 MAPK may be involved in NF-κB activation [35]. Indeed, we found that a specific NF-κB-blocking peptide (SN18) was only partially able to antagonize lovastatin-induced apoptosis, probably because of the sensitization to apoptosis mediated per se by NF-κB blockade [36].

The antitumoral activity of lovastatin was assessed in vivo on the growth of tumors generated by FRTL-5-K-Ras s.c. cell injection in nude mice. The dramatic effect observed in the treated group recommended further investigations on other benign or malignant thyroid proliferative diseases. It is important to note that lovastatin is able to exert apoptotic and differentiation effects against anaplastic thyroid carcinoma cell lines. We have recently shown that lovastatin treatment significantly increased the effects of the oncolytic virus dl1520 against ATC cells [37]. In this cellular model, the replication of dl1520 was enhanced by lovastatin treatment, and a significant increase of the expression of the early gene E1A 13 S and the late gene Penton was observed in lovastatin-treated cells. Finally, lovastatin treatment significantly enhanced the effects of dl1520 against ATC tumor xenografts [37].

Both tumor and transformed cells are usually more resistant to oxidative stress with respect to normal cells [38]. This peculiarity could interfere with the efficacy of antitumor therapy based on free radical generation like radiotherapy or chemotherapy with various drugs. Therefore, the finding of new therapeutic targets able to enhance free-radical-mediated damage in tumor cells is of increasing interest. Moreover, the present report is one of the first demonstrations that K-ras targeting could be a useful tool to increase oxidative stress in thyroid cancer and the latter effect induces modulation of multiple signals (ERK, NF-κB, p38 kinase) that could represent additional therapeutic targets in integrated anticancer strategies. In conclusion, the differential sensitivity of K-ras-transformed thyroid cells to inhibitors of prenylation with respect to induction of apoptosis could be a solid ground to build therapeutic strategies for those proliferative diseases sustained by an inappropriate K-ras expression.

Acknowledgments This work was supported by the Italian Association for Cancer Research (AIRC) and by the Associazione Educazione e Ricerca Medica Salernitana. Simona Pisanti was supported by a fellowship from FIRC. We thank Prof. Maria Caterina Turco, Department of Pharmaceutical Sciences, University of Salerno, Dr. Maria Rosaria Santillo and Dr. Rosalba Serù, Department of Neuroscience, University of Naples Federico II, Italy, for useful discussion and technical assistance.

References

1. Downward J (2003) Targeting RAS signalling pathways in cancer therapy. Nat Rev Cancer 3:11–22
2. Wittinghofer A, Nassar N (1996) How Ras-related proteins talk to their effectors. Trends Biochem Sci 21:488–491
3. Rassool FV, Gaymes TJ, Omidvar N, Brady N, Beurlet S, Pla M, Reboul M, Lea N, Chomienne C, Thomas NS, Mufti GJ, Padua RA (2007) Reactive oxygen species, DNA damage, and error-prone repair: a model for genomic instability with progression in myeloid leukemia? Cancer Res 67(18):8762–8771
4. Santillo M, Mondola P, Serù R, Annella T, Cassano S, Ciullo I, Tecce MF, Iacomino G, Damiano S, Cuda G (2001) Opposing functions of Ki- and Ha-Ras genes in the regulation of redox signals. Current Biology 11:614–619

5. Casey PJ, Solski PA, Der CJ, Buss JE (1989) p21ras is modified by a farnesyl isoprenoid. Proc Natl Acad Sci USA 86:8323–8327
6. Hancock JF, Magee AI, Childs JE, Marshall CJ (1989) All ras proteins are polyisoprenylated but only some are palmitoylated. Cell 57:1167–1177
7. Trahey M, McCormick F (1987) A cytoplasmic protein stimulates normal N-ras p21 GTPase, but does not affect oncogenic mutants. Science 238:542–545
8. Kondo T, Ezzat S, Asa SL (2006) Pathogenetic mechanisms in thyroid follicular-cell neoplasia. Nat Rev Cancer 6(4):292–306
9. Laezza C, Di Marzo V, Bifulco M (1998) v-K-ras leads to preferential farnesylation of p21(ras) in FRTL-5 cells: multiple interference with the isoprenoid pathway. Proc Natl Acad Sci USA 95:13646–13651
10. Caraglia M, Budillon A, Tagliaferri P, Marra M, Abbruzzese A, Caponigro F (2005) Isoprenylation of intracellular proteins as a new target for the therapy of human neoplasms: preclinical and clinical implications. Curr Drug Targets 6:301–323
11. Caraglia M, Santini D, Marra M, Vincenti B, Tonini G, Budillon A (2006) Emerging anti-cancer molecular mechanisms of aminobisphosphonates. Endocr Rel Cancer 13:7–26
12. Agarwal B, Bhendwal S, Halmos B, Moss SF, Ramey WG, Holt PR (1999) Lovastatin augments apoptosis induced by chemotherapeutic agents in colon cancer cells. Clin Cancer Res 5:2223–2229
13. Zhong WB, Liang YC, Wang CY, Chang TC, Lee WS (2005) Lovastatin suppresses invasiveness of anaplastic thyroid cancer cells by inhibiting Rho geranylgeranylation and RhoA/ROCK signaling. Endocr Relat Cancer 12:615–629
14. Yao CJ, Lai GM, Chan CF, Cheng AL, Yang YY, Chuang SE (2006) Dramatic synergistic anticancer effect of clinically achievable doses of lovastatin and troglitazone. Int J Cancer 118: 773–779
15. Wong WW, Clendening JW, Martirosyan A, Boutros PC, Bros C, Khosravi F, Jurisica I, Stewart AK, Bergsagel PL, Penn LZ (2007) Determinants of sensitivity to lovastatin-induced apoptosis in multiple myeloma. Mol Cancer Ther 6:1886–1897
16. Vitale M, Di Matola T, Rossi G, Laezza C, Fenzi G, Bifulco M (1999) Prenyltransferase inhibitors induce apoptosis in proliferating thyroid cells through a p53-independent CrmA-sensitive, and caspase-3-like protease-dependent mechanism. Endocrinology 140:698–704
17. D'Acquisto F, de Cristofaro F, Maiuri MC, Tajana G, Carnuccio R (2001) Protective role of nuclear factor kappa B against nitric oxide-induced apoptosis in J774 macrophages. Cell Death Differ 8:144–151
18. Bifulco M, Laezza C, Aloj SM (1999) Inhibition of farnesylation blocks growth but not differentiation in FRTL-5 thyroid cells. Biochimie 81:287–290
19. Fusco A, Pinto A, Ambesi-Impiombato FS, Vecchio G, Tsuchida N (1981) Transformation of rat thyroid epithelial cells by Kirsten murine sarcoma virus. Int J Cancer 28:655–662
20. Fusco A, Portella G, Di Fiore PP, Berlingieri MT, Di Lauro R, Schneider AB, Vecchio G (1985) A mos oncogene-containing retrovirus, myeloproliferative sarcoma virus, transforms rat thyroid epithelial cells and irreversibly blocks their differentiation pattern. J Virol 56:284–292
21. Colletta G, Pinto A, Di Fiore PP, Fusco A, Ferrentino M, Avvedimento VE, Tsuchida N, Vecchio G (1983) Dissociation between transformed and differentiated phenotype in rat thyroid epithelial cells after transformation with a temperature-sensitive mutant of the Kirsten murine sarcoma virus. Mol Cell Biol 3:2099–2109
22. McAnally JA, Gupta J, Sodhani S, Bravo L, Mo H (2007) Tocotrienols potentiate lovastatin-mediated growth suppression in vitro and in vivo. Exp Biol Med 232:523–531
23. Shibata MA, Kavanaugh C, Shibata E, Abe H, Nguyen P, Otsuki Y, Trepel JB, Green JE (2003) Comparative effects of lovastatin on mammary and prostate oncogenesis in transgenic mouse models. Carcinogenesis 24:453–459
24. Nomura K, Imai H, Koumura T, Arai M, Nakagawa Y (1999) Mitochondrial phospholipid hydroperoxide glutathione peroxidase suppresses apoptosis mediated by a mitochondrial death pathway. J Biol Chem 274:29294–29302
25. Takahashi A, Masuda A, Sun M, Centonze VE, Herman B (2004) Oxidative stress-induced apoptosis is associated with alterations in mitochondrial caspase activity and Bcl-2-dependent alterations in mitochondrial pH (pHm). Brain Res Bull 62:497–504
26. Szatrowski TP, Nathan CF (1991) Production of large amounts of hydrogen peroxide by human tumor cells. Cancer Res 51:794–798
27. Toyokuni S, Okamoto K, Yodoi J, Hiai H (1995) Persistent oxidative stress in cancer. FEBS Lett 358:1–3
28. Mitsushita J, Lambeth JD, Kamata T (2004) The superoxidegenerating oxidase Nox1 is functionally required for Ras oncogene transformation. Cancer Res 64:3580–3585
29. Qi X, Tang J, Pramanik R, Schultz RM, Shirasawa S, Sasazuki T, Han J, Chen G (2004) p38 MAPK activation selectively induces cell death in K-ras-mutated human colon cancer cells through regulation of vitamin D receptor. J Biol Chem 279:22138–22144
30. Dolado I, Swat A, Ajenjo N, De Vita G, Cuadrado A, Nebreda AR (2007) p38alpha MAP kinase as a sensor of reactive oxygen species in tumorigenesis. Cancer Cell 11:191–205
31. Motohashi H, Yamamoto M (2004) Nrf2-Keap1 defines a physiologically important stress response mechanism. Trends Mol Med 10:549–557
32. Zhu H, Itoh K, Yamamoto M, Zweier JL, Li Y (2005) Role of Nrf2 signaling in regulation of antioxidants and phase 2 enzymes in cardiac fibroblasts: protection against reactive oxygen and nitrogen species-induced cell injury. FEBS Lett 579:3029–3036
33. Scorziello A, Santillo M, Adornetto A, Dell'aversano C, Sirabella R, Damiano S, Canzoniero LM, Renzo GF, Annunziato L (2007) NO-induced neuroprotection in ischemic preconditioning stimulates mitochondrial Mn-SOD activity and expression via Ras/ERK1/2 pathway. J Neurochem 103:1472–1480
34. Barkett M, Gilmore TD (1999) Control of apoptosis by Rel/NfkB transcription factors. Oncogene 18:6910
35. Vanden Berghe W, Plaisance S, Boone E, De Bosscher K, Schmitz ML, Fiers W, Haegeman G (1998) p38 and extracellular signal-regulated kinase mitogen-activated protein kinase pathways are required for nuclear factor-kB p65 transactivation mediated by tumor necrosis factor. J Biol Chem 273:3285–3290
36. Wang X, Chen W, Lin Y (2007) Sensitization of TNF-induced cytotoxicity in lung cancer cells by concurrent suppression of the NF-kappa B and Akt pathways. Biochem Biophys Res Commun 355:807–812
37. Libertini S, Iacuzzo I, Ferraro A, Vitale M, Bifulco M, Fusco A, Portella G (2007) Lovastatin enhances the replication of the oncolytic adenovirus dl1520 and its antineoplastic activity against anaplastic thyroid carcinoma cells. Endocrinology 148: 5186–5194
38. Martindale JL, Holbrook NJ (2002) Cellular response to oxidative stress: signaling for suicide and survival. J Cell Physiol 192:1–15